

Scientific paper

# Synthesis, Characterization, Cytotoxicity and DNA Binding Studies of a nNovel Anionic Organopalladium(II) Complex

Maryam Saeidifar,<sup>1,\*</sup> Hassan Mansouri-Torshizi,<sup>2</sup> Y. Palizdar,<sup>1</sup>  
M. Eslami-Moghaddam,<sup>3</sup> Adeleh Divsalar<sup>4</sup> and Ali Akbar Saboury<sup>5</sup>

<sup>1</sup> Department of Nanotechnology and Advanced Materials, Materials and Energy Research Center, Karaj, Iran

<sup>2</sup> Department of Chemistry, University of Sistan and Baluchestan, Zahedan, Iran

<sup>3</sup> Chemistry and Chemical Engineering Research Center, Tehran, Iran

<sup>4</sup> Department of Cell and Molecular Biology, Faculty of Biological Sciences, Kharazmi University, Tehran, Iran

<sup>5</sup> Institute of Biochemistry and Biophysics, University of Tehran, Tehran, Iran

\* Corresponding author: E-mail: saeidifar@merc.ac.ir

Tel: +98 26 36280040; Fax: +98 26 36201888.

Received: 28-10-2013

## Abstract

A new anionic 8-hydroxyquinolinatopalladate(II) complex with malonate has been synthesized and characterized by elemental analysis, conductivity, FT-IR, UV-Vis and <sup>1</sup>H NMR techniques to enhance the development of potential anti-cancer agents. Cytotoxicity was determined against the human leukemia cells, Molt-4, by MTT assay. The novel antitumor Pd(II) complex was evaluated for its binding to calf thymus DNA (ctDNA) in physiological buffer (pH 7.0) by using absorption spectroscopy, fluorescence titration spectra, ethidium bromide displacement and gel chromatography studies. The results obtained from these analyses indicated that the water-soluble complex can bind to DNA cooperatively through a static quenching procedure at low concentrations. Thermodynamic parameters obtained from fluorescence experiments at different temperatures revealed the hydrogen binding and van der Waals force in the binding process which was supported by Scatchard's plots.

**Keywords:** DNA-binding; anionic complex; 8-hydroxyquinoline; malonate; cytotoxicity

## 1. Introduction

Deoxyribonucleic acid (DNA) is an important genetic substance in the organism, which plays an extremely significant role in the process of human life, such as gene expression, gene transcription, mutagenesis, and carcinogenesis.<sup>1,2</sup> DNA is quite often the main molecular target for studies with pollutants. Many pollutants exert their carcinogenic action and teratogenic action by mutating the DNA. The pollutants, which either covalently bind or intercalate in DNA molecule and form DNA adducts may lead to gene mutations and initiate carcinogenesis, if the adducts are not repaired or misrepaired before DNA repli-

cation occurs.<sup>3,4</sup> The study on the interaction between small molecules and DNA has been the focus of some recent research in the scope of life science, chemistry, clinical medicine and genetics. These studies are very useful for investigating the structure and biological function of DNA, and elucidating the damage mechanism of DNA.

Generally, the molecular forces contributing to biomolecules interactions with small molecules substrates may involve hydrogen bond, van der Waals force, hydrophobic interaction force, and electrostatic force.<sup>1,5,6</sup> Palladium organometallic compounds exhibit interesting biological and pharmacological properties.<sup>7,8,9,10,11–12</sup> Because of its therapeutic effects, the study of the interaction of these complexes with DNA is important both of under-

standing molecular mechanism of the drug action and contributing to the design of several DNA-targeted drugs.

Many methods have been employed to investigate the interaction of small molecules with DNA: spectroscopic techniques, nuclear magnetic resonance (NMR), agarose gel electrophoresis, X-ray diffraction, viscosity measurement, melting measurement and electrochemical measurements, etc.<sup>13,14–15</sup> Among these methods, spectroscopic methods are common because of their sensitivity, rapidity, simpleness, reproducibility and convenience.<sup>13,16,17,13</sup>

In the present work, the design, synthesis and characterization of a new anionic palladium(II) complex bearing 8-hydroxyquinoline and malonate as chelating ligands has been reported. Study of the cytotoxic activity in vitro of the complex has been exerted. The binding mechanism of the water-soluble palladium(II) complex to calf thymus DNA under simulated physiological conditions (pH 7.0) has also been investigated by UV-Vis spectroscopy, fluorescence measurements and gel chromatography. The challenge here was the interaction between an anionic complex and ctDNA with the anionic sugar-phosphate backbone that has been reported for the first time. These results may throw light on the interaction mechanisms of this type of complexes with DNA of cells and possible side effects of this agent. Moreover, to quantitatively analyze the interaction between the palladium complex and DNA, the relative thermodynamic characteristics were estimated.

## 2. Experimental

### 2.1. Materials and Methods

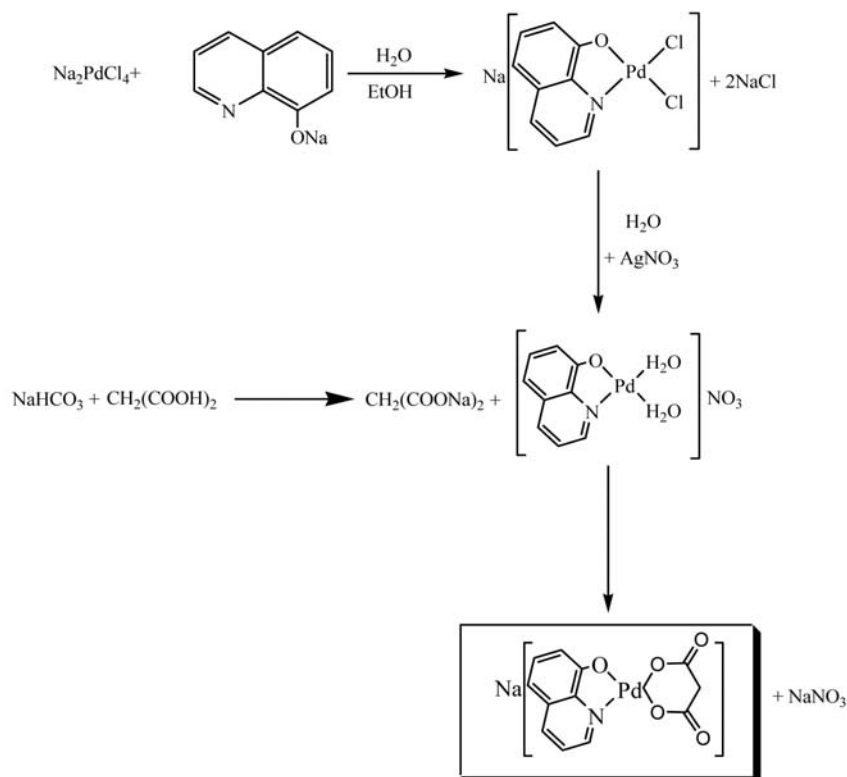
Palladium(II) chloride anhydrous and sodium chloride were obtained from Fluka (Switzerland). 8-hydroxyquinoline, sodium bicarbonate, silver nitrate, sephadex G-25, malonic acid and tris(hydroxymethyl) amino methane hydrochloride (Tris-HCl buffer) were obtained from Merck (Germany). Calf thymus DNA (ctDNA) and ethidium bromide (EB) were obtained from Sigma Chemical Co. (USA) and used as received. The stock solutions of Pd(II) complex (1 mM) was made in Tris-HCl buffer by gentle stirring and heating at 308 K and the stock solution of ctDNA (4 mg/mL) was prepared by dissolving of ctDNA in 20 mM NaCl- 20 mM Tris-HCl buffer at pH 7.0 overnight and was stored at 277 K for about a week. The ctDNA concentration per nucleotide was determined by absorption spectroscopy using the molar absorption coefficient ( $6600 \text{ M}^{-1} \text{ cm}^{-1}$ ) at 260 nm.<sup>18,19</sup> Solutions of ctDNA gave a ratio of UV-Vis absorbance of 1.8–1.9 : 1 at 260 and 280 nm, indicating that the ctDNA was sufficiently free of protein.<sup>18</sup> The cell line for the cytotoxicity studies was obtained from the Cell Bank of Pasteur Institute in Tehran (IRAN). Solvents were used of reagent grade and purified before being used by the standard met-

hods. Double-distilled water was used as solvent. All the experiments repeated to get the constant results.

The melting point of the complex was determined on a Unimelt capillary melting point apparatus and reported uncorrected. Conductivity measurement of the complex was carried out on a Systronics conductivity bridge 305, using a conductivity cell of cell constant 1.0. Infrared spectrum ( $4000\text{--}400 \text{ cm}^{-1}$ ) was determined with KBr disk on a JASCO-460 plus FT-IR spectrophotometer. <sup>1</sup>H NMR spectrum was measured on a Bruker DRX-500 Avance spectrometer at 500 MHz, using TMS as the internal reference in DMSO-d<sub>6</sub>. UV-Vis spectrum was recorded on a Perkin-Elmer lambda-25 recording spectrophotometer. Fluorescence intensity changes were studied by using a Hitachi spectrofluorimeter, MPF-4 model, equipped with a thermostatically controlled cuvette compartment. The following spectrometric measurements were all performed in a quartz cuvette of 1 cm path length.

### 2.2. Synthesis of Sodium 8-hydroxyquinolinatomalonatopalladate(II) (Na[Pd(8-QO)(mal)])

NaCl (118 mg, 2 mmol) was added to a solution of PdCl<sub>2</sub> (177 mg, 1 mmol) in distilled water (20 mL) and the reaction mixture was stirred at 333–343 K until a light brown solution formed. In a separate beaker, 8-QOH (145 mg, 1 mmol) was dissolved in distilled water and ethanol mixture (1 mL, 1:1 v/v) followed by adding NaHCO<sub>3</sub> (84 mg, 1 mmol) and then the solution stirred at 313 K until a light yellow solution formed. A light yellow solution of 8-QONa (1 mmol), was added dropwise to a light brown solution of Na<sub>2</sub>PdCl<sub>4</sub> (1 mmol) in distilled water (100 mL) under stirring at room temperature and the color of the mixture changed to dark green. Then the mixture was stirred for 30 minutes at 313 K. AgNO<sub>3</sub> (340 mg, 2 mmol) was added to Na[Pd(8-QO)Cl<sub>2</sub>] solution and stirred in the dark at 328 K for 6 h and then overnight at room temperature that resulted in yellow-orange solution containing [(8-QO)Pd(H<sub>2</sub>O)<sub>2</sub>]NO<sub>3</sub>. The AgCl precipitate was filtered off by using Whatman 42 filter paper. CH<sub>2</sub>(CO<sub>2</sub>Na)<sub>2</sub> (104 mg, 1 mmol) solution was slowly added to the clear yellow-orange [(8-QO)Pd(H<sub>2</sub>O)<sub>2</sub>]NO<sub>3</sub> (1 mmol), which was formed at the previous stage. CH<sub>2</sub>(CO<sub>2</sub>Na)<sub>2</sub> was prepared by adding NaHCO<sub>3</sub> (170 mg, 2 mmol) to CH<sub>2</sub>(CO<sub>2</sub>H)<sub>2</sub> (104 mg, 1 mmol). The yellow mixture was stirred for 3 h at 313–323 K. During the heating the volume of the solution reduced to 25 mL and the solution cooled down to be filtered again. Then, the solution was heated at 308–313 K until the dried yellow powder was obtained. The residue was dissolved in acetonitril-methanol (1:1 v/v, 10 mL) and then evaporated at 308–313 K to complete dryness. Recrystallization was carried out by stirring the crude product in mixture of methanol-acetonitrile (1:1 v/v, 10 mL) followed by filtering the undissolved particles. Diffusion of ether into the precipitate for three days resulted in a



Scheme 1. The Syntheses route of Na[Pd(8-QO)(mal)] complex.

yellow powder. The powder that were isolated by filtration, washed with ether and dried at 313 K. The preparation steps of Sodium 8-hydroxyquinolinatomalonatopalladate(II) are shown in Scheme 1. Yield: 0.269 g (72%) and decomposes at 471–472 K. Anal. Calc. for  $\text{NaC}_{12}\text{H}_8\text{NO}_5\text{Pd}$  (375): C, 34.78; H, 1.93; N, 6.76%. Found: C, 34.75; H, 1.90; N, 6.79%. Molar conductance,  $\Lambda_M$  ( $10^{-4}$  M,  $\text{H}_2\text{O}$ ) =  $125 \Omega^{-1} \text{cm}^2 \text{mol}^{-1}$ . FT-IR (KBr)  $\text{cm}^{-1}$ : 585–595, 1112, 1321, 1470, 1644, 166, 1904  $\text{cm}^{-1}$ . UV  $\lambda_{\text{max}}$  ( $\text{H}_2\text{O}$ ) nm ( $\epsilon$ ): 376 (0.19), 249 (1.16);  $^1\text{H}$  NMR (500 MHz,  $\text{DMSO}-d_6$ , TMS)  $\delta$ : 3.43 (s, 2H, H-a), 6.72 (d,  $J = 7.85$  Hz, 1H, H-6), 6.97 (d,  $J = 2.05$  Hz, 1H, H-4), 7.34 (t,  $J = 7.92$  Hz, 1H, H-2), 7.54 (dd,  $J = 4.95$  Hz, 1H, H-5), 7.96 (d,  $J = 4.2$  Hz, 1H, H-3), 8.44 (d,  $J = 8.25$  Hz, 1H, H-1).

### 2. 3. In Vitro Cytotoxicity Studies

Cell proliferation was evaluated by using a system based on the tetrazolium compound [3-(4,5-dimethylthiazol-2-yl)-2,5-diphenyltetrazolium bromide, MTT] that is reduced by living cells to yield a soluble formazan product which can be assayed colorimetrically.<sup>20–21</sup> The MTT assay is dependent on the cleavage and conversion of the soluble yellowish MTT to the insoluble purple formazan by active mitochondrial dehydrogenase of living cells. The human leukemia cells, molt, was maintained in a RPMI medium supplemented with 10% heat-inactivated fetal calf serum and 2 mM L-glutamine, streptomycin and pe-

nicillin (5  $\mu\text{g}/\text{mL}$ ), at 310 K under a 5%  $\text{CO}_2$ /95% air atmosphere. Harvested cells were seeded into 96-well plates ( $2 \cdot 10^4$  cell/mL) with varying concentrations of the sterilized complex (0–250  $\mu\text{M}$ ) and incubated for 48 hours. At the end of the four hour incubation period, 25  $\mu\text{L}$  of MTT solution (5 mg/mL in PBS) was added to each well containing fresh culture media.<sup>13</sup> The insoluble produced formazan was then dissolved in solution containing 10% SDS and 50% DMF (under dark condition for 2 h at 310 K), and optical density (OD) was read against reagent blank with a multiwell scanning spectrophotometer (ELISA reader, Model Expert 96, Asys Hitchtech, Austria) at a wavelength of 570 nm. Absorbance is read as a function of concentration of converted dye. The OD value of study groups was divided by the OD value of untreated control and presented as a percentage of the control (as 100%). Results were analyzed for statistical significance using a two-tailed Student's t-test. Changes were considered significant at  $p < 0.05$ . In this experiment, the clear stock solution (2 mM, in deionized water) was sterilized by filtering through sterilizing membrane (0.1  $\mu\text{m}$ ) and then varying concentrations of the sterilized complex (0–25  $\mu\text{M}$ ) were added to harvested cells.

### 2. 4. UV-Vis Absorbance Measurement

The UV-visible absorption spectra were recorded at 260 nm and at 640 nm to eliminate the interference of

turbidity. The concentration of ctDNA was constant (14  $\mu\text{M}$ ) while the complex concentrations was from 5.5 to 298  $\mu\text{M}$  and 5.5 to 277  $\mu\text{M}$  at 300 K and 310 K, respectively. Thus, addition of metal complex was continued until no further changes in the absorption readings were observed. Also, to obtain the maximum  $\Delta A$  ( $\Delta A_{\text{max}}$ ), change in the absorbance when all binding sites on ctDNA were occupied by metal complex, the successive fixed amount of the complex solution (200  $\mu\text{M}$ ) was added to ctDNA solution (62–103  $\mu\text{M}$  and 67–108  $\mu\text{M}$  at 300 K and 310 K, respectively). In addition, to affirm quantitatively the affinity of the complex bound to ctDNA, a fixed amount of ctDNA (51.5  $\mu\text{M}$ ) was titrated with varying concentrations of the complex (90–180  $\mu\text{M}$  and 100–155  $\mu\text{M}$  at 300 K and 310 K, respectively). The binding parameters (Hill coefficient,  $n$ , apparent binding constant,  $K$  and number of binding sites per 1000 nucleotides of ctDNA,  $g$ ) of metal complex to ctDNA were obtained.

## 2. 5. Fluorescence Spectral Measurements

A quantitative analysis of affinity interaction between Pd(II) complex and ctDNA was carried out by the luminescence titration method at 293 K, 300 K and 310 K. A fixed solution of ctDNA and ethidium bromide was titrated by appropriate amount of Pd(II) complex solution. The concentration range of complex was 0 to 1.33  $\mu\text{M}$  and the concentration of ctDNA and EB were kept at 60  $\mu\text{M}$  and 2  $\mu\text{M}$ , respectively.

To characterize the mode of binding of Pd(II) to ctDNA, the Pd(II) complex were incubated with ctDNA at room temperature for 4 hours. The appropriate amount of EB was added before an additional incubation at 298 K for 2 hours before the fluorescence spectral measurement. Saturation curves of fluorescence intensity for [Pd(8-QO)(mal)]<sup>-</sup>-DNA system at different  $r_f$  values (3.33, 6.67 and 10.0) were obtained in the presence of increased concentrations of EB (2, 4, ..., 20  $\mu\text{M}$ ). The emission spectra of both measurements were recorded in the emission wavelength range of 540–700 nm with an excitation wavelength at 471 nm. The widths of both the excitation slit and emission slit were set at 5.0 nm. The fluorescence spectra of the Pd(II) complex at the highest denaturant concentration at 471 nm excitation wavelength have been checked, and the emission intensities of these compounds were very small and negligible.

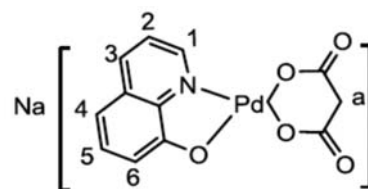
## 2. 6. Mode of Binding

The Pd(II) complex (337.5  $\mu\text{M}$ ) was incubated with calf thymus DNA (187.5  $\mu\text{M}$ ) for 4 h at 301 K in Tris-HCl buffer (pH 7.0). It was then passed through a Sephadex G-25 column equilibrated with the same buffer. The elution of the column fraction of 2.0 mL was monitored at 376 nm and 260 nm for DNA-Pd(II) complex.

## 3. Results and Discussion

### 3. 1. Synthesis and Characterization of the Complex

The palladium(II) complex has been synthesized and reported in the experimental section. The complex is soluble in water and stable to air and moisture without any kind of decomposition also after several months. The complex has been characterized by elemental analysis, molar conductivity measurements and FT-IR, UV-Visible and <sup>1</sup>H NMR spectroscopic techniques. All the results are in good agreement with the proposed structure of the complex. The molar conductance of the complex (10<sup>-4</sup> M) in water was 125  $\Omega^{-1} \text{mol}^{-1} \text{cm}^2$ . It was within the range of 118 to 131  $\text{cm}^2 \text{ohm}^{-1} \text{mol}^{-1}$  which is in conformity for 1:1 electrolytic natures. Solid state FT-IR spectroscopy of the complex shows four main characteristic bands at 1112, 1321 and 1644 and 1470  $\text{cm}^{-1}$  assigned to  $\nu(\text{C}-\text{O})$ ,  $\nu(\text{N}-\text{C})$  and  $\nu(\text{C}=\text{C})_{\text{aromatic}}$  modes respectively. The observed  $\nu(\text{COO}^-)$  at 1661  $\text{cm}^{-1}$  and  $\nu(\text{C}-\text{H})_{\text{aliphatic}}$  at 1904  $\text{cm}^{-1}$  in comparison with free ligand suggests the coordination of malonate to palladium center through their oxygens.<sup>23,24</sup> The complex shows bands within the range 585–595  $\text{cm}^{-1}$  and 470–490  $\text{cm}^{-1}$  may be assignable to the  $\nu(\text{M}-\text{N})$  and  $\nu(\text{M}-\text{O})$ , respectively.<sup>25,26</sup> Two absorption bands with varied intensity were observed in both of the UV and visible region. The band at 376 nm ( $\epsilon = 0.19$ ) is assigned to metal to  $\pi^*$  orbital of 8-hydroxyquinoline charge transfer. Besides, a band was also observed at 249 nm ( $\epsilon = 1.16$ ), corresponding to the internal  $\pi \rightarrow \pi^*$  transitions of 8-hydroxyquinoline ligand.<sup>27</sup> The later bands generally show overlapping and therefore it is not possible to assign them properly. The <sup>1</sup>H NMR spectrum (Fig. S1 Supplementary data file) of the complex in DMSO-*d*<sub>6</sub> exhibited signal at the doublet observed at 6.72 ppm, 6.97 ppm, 7.96 ppm and 8.44 ppm, the triplet at 7.34 ppm and a quartet at 7.54 ppm are assigned to H-6, H-4, H-3, H-1, H-2 and H-5 protons, respectively. The signal



**Scheme 2.** Proposed structures and proton nmr numbering schemes of Na[Pd(8-QO)(mal)] complex.

due to the H-a protons appears a singlet at 3.43. The NMR numbering scheme are given in scheme 2.

### 3. 2. Cytotoxic Activity

The effect of prepared complex on human leukemia cell lines, molt, was evaluated by MTT assay. As shown

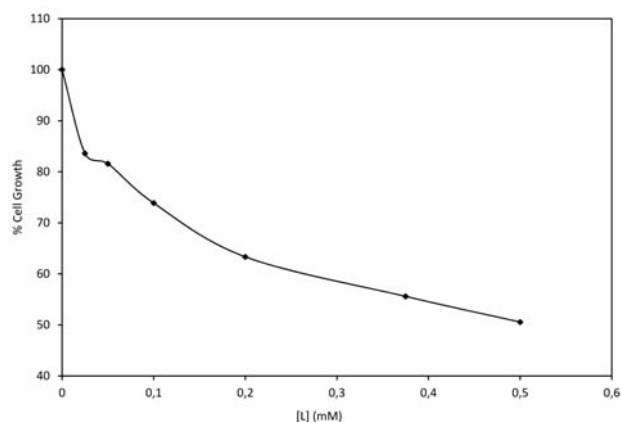


**Fig. 1.** The growth suppression activity of the Na[Pd(8-QO)(mal)] complex on T47D cell line.

In Figure 1, the number of growing cells was significantly reduced after 48 hours in the presence of various concentrations of the palladium complex. The  $IC_{50}$  value of the Na[Pd(8-QO)(mal)] is  $0.5 \pm 0.2$  mM, that is comparable with those of cationic Pd(II) complexes reported earlier.<sup>28,29</sup> These results suggest that the Pd(II) complex shows moderate activity and may be potential antitumor agent.

### 3. 3. UV-Vis Spectroscopy Studies

UV-Vis absorption measurement is a very simple and applicable method to investigate structural changes and complex formations.<sup>30,31</sup> Figure 2 shows the results of UV-Vis spectrum analysis of ctDNA in the presence of complex at 300 and 310 K. The concentration of the metal complex at midpoint of transition,  $[L]_{1/2}$ , according to the denaturation plots is 0.190 mM at 300 K and 0.182 mM at 310 K. These values were mentioned that the complex can bind to ctDNA at low concentrations comparable with cationic complexes.<sup>29,30,32</sup> Thus, if the complex will be used

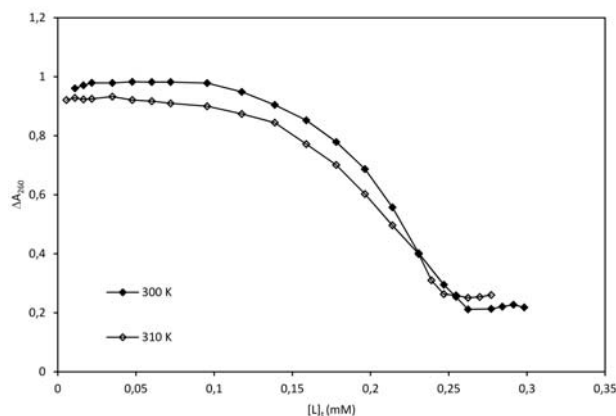


**Fig. 2.** The absorbance changes of DNA in Tris-HCl buffer at  $\lambda_{\text{max}} = 260$  nm in the presence of increasing amounts of Na[Pd(8-QO)(mal)] complex,  $[L]_i$ , at 300 K and 310 K.

as anti-tumor agents, low doses will be needed, which may have fewer side effects.

The values of unfolding equilibrium constant,  $K$ , and unfolding free energy,  $\Delta G^\circ$ , of ctDNA in the presence of Pd(II) complex have been calculated using the Figure 2 and Pace method.<sup>33</sup> In this method, Pace had assumed two-state mechanism, nature and denature, and then calculated unfolding free energy of ctDNA by using Equations 1 and 2:

$$K = (A_N - A_{\text{obs}}) / (A_{\text{obs}} - A_D) \quad (1)$$

$$\Delta G^\circ = -RT \ln K \quad (2)$$

Where  $A_{\text{obs}}$  is absorbance readings in transition region,  $A_N$  and  $A_D$  are absorbance readings of nature and denatured conformation of ctDNA, respectively. A straight line is observed when the values of  $\Delta G^\circ$  are plotted against the concentrations of the metal complex in the transition region at 300 K and at 310 K (Fig. 3). The equation for these lines can be written as follow.<sup>34</sup>

$$\Delta G^\circ = \Delta H^\circ_{(\text{H}_2\text{O})} - m [L]_i \quad (3)$$

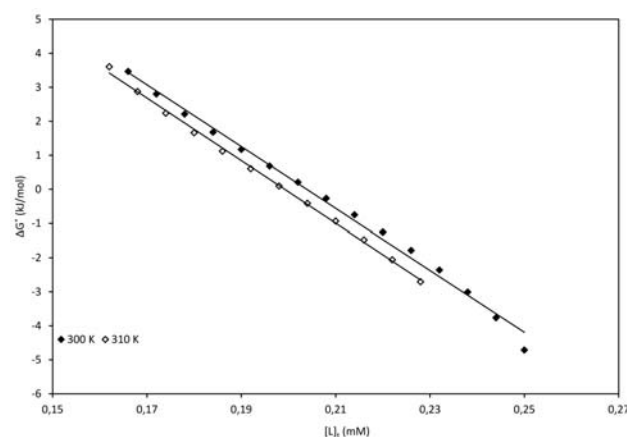


**Fig. 3.** The molar Gibbs free energy changes of interaction between ctDNA and Na[Pd(8-QO)(mal)] complex.

Here the values of  $\Delta H^\circ_{(\text{H}_2\text{O})}$  for each curve are measured from the intercept on ordinate of the plots and it is conformational stability of ctDNA in the absence of metal complex. The values of  $\Delta G^\circ$  (Table 1) are decreased by increasing the temperature because of decreasing in ctDNA stability.<sup>35</sup> The metal complex ability to interact with ctDNA,  $m$ , was measured from the slope of each curve in Figure 3. The values of  $m$  for the palladium complex are much higher than those of Pd(II) complexes reported earlier.<sup>29,30</sup> which indicate the higher ability of the complex to interaction with ctDNA. Another important thermodynamic parameter found is the molar enthalpy of ctDNA denaturation in absence of metal complexes,  $\Delta H^\circ_{(\text{H}_2\text{O})}$ . The molar enthalpy of ctDNA denaturation in the presence of

metal complex,  $\Delta H^\circ_{\text{conformation}}$ , in the range of the two temperatures was calculated using Gibbs-Helmholtz equation.<sup>36</sup>

$$\Delta H^\circ = (\Delta G^\circ_{(T_1)}/T_1 - \Delta G^\circ_{(T_2)}/T_2) / (1/T_1 - 1/T_2) \quad (4)$$

Upon plotting the values of these enthalpies versus the concentrations of metal complex, straight lines were obtained as shown in Fig. 4 for this complex. Intraprojection of this line (intercept on ordinate i.e. absence of metal complex) gives the value of  $\Delta H^\circ_{(H_2O)}$  (Table 1). The decreasing of enthalpy change with increasing concentrations of this complex indicated that the stability of ctDNA had been decreased. In addition, it can be concluded that the interaction of Pd(II) complex with ctDNA is exothermic.<sup>37</sup> Generally, Gibbs free energy and enthalpy decrease with increasing concentration of Pd(II) complex. Thus, Pd(II) complex binding to ctDNA is spontaneous reaction and in presence of this complex enthalpy is favorable.

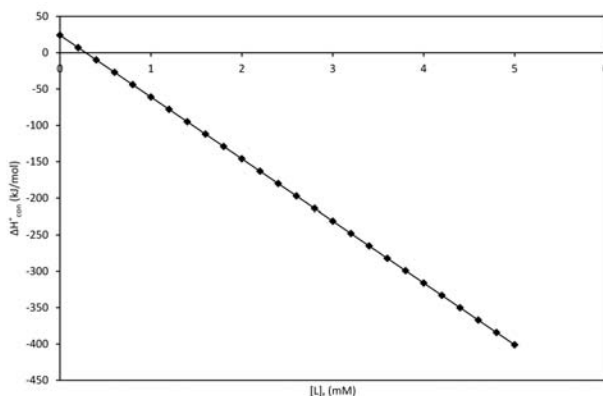


Fig. 4. The molar enthalpy of interaction between ctDNA and Na[Pd(8-QO)(mal)] complex in the range of 300 K to 310 K.

For calculating of binding parameters, change in absorbance,  $\Delta A$ , was calculated by subtracting the absorbance reading of mixed solutions of the metal complex with various concentrations of ctDNA, from absorbance reading of free metal complex. The maximum  $\Delta A$  ( $\Delta A_{\text{max}}$ ) of the metal complex totally bound to ctDNA was determined by intraprojection of a plot of reciprocal of  $\Delta A$  against the reciprocal of ctDNA concentration (i.e. intercept on ordinate) (Fig. S2 Supplementary data file). The values of  $\Delta A_{\text{max}}$  are given in Table 2. Titration of fixed amount of ctDNA with varying amount of the metal complex was ob-

tained the concentration of the metal complex bound to ctDNA,  $[L]_b$ , using the Equation 5.<sup>38</sup>

$$[L]_b = \Delta A [L]_t / \Delta A_{\text{max}} \quad (5)$$

Where  $[L]_t$  is the total concentration of metal complex. The concentration of the free metal complex,  $[L]_f$ , and the ratio of the concentration of bound metal complex to the total ctDNA concentration,  $\nu$ , can be calculated from Equation 6 and Equation 7, respectively.

$$[L]_f = [L]_t - [L]_b \quad (6)$$

$$\nu = [L]_b / [DNA]_t \quad (7)$$

The Scatchard plots were obtained separately at 300 K and 310 K by plotting  $\nu/[L]_f$  versus  $\nu$  (Fig. 5).<sup>39</sup> From the nature of the plot, the type of cooperativity can be verified (concave downward curve indicates cooperative, concave upward anti-cooperative and straight line non cooperative). These plots are curvilinear concave downwards, suggesting cooperative binding.<sup>40</sup> To obtain the binding parameters, the above experimental data ( $\nu$  and  $[L]_f$ ) were substituted in Equation 8, i. e. Hill equation.<sup>40</sup>

$$\nu = g(K[L]_f)^n / (1 + (K[L]_f)^n) \quad (8)$$

This equation contain the following unknown parameters  $n$ ,  $K$  and  $g$  where  $n$  is the Hill coefficient ( $n = 1$  in-

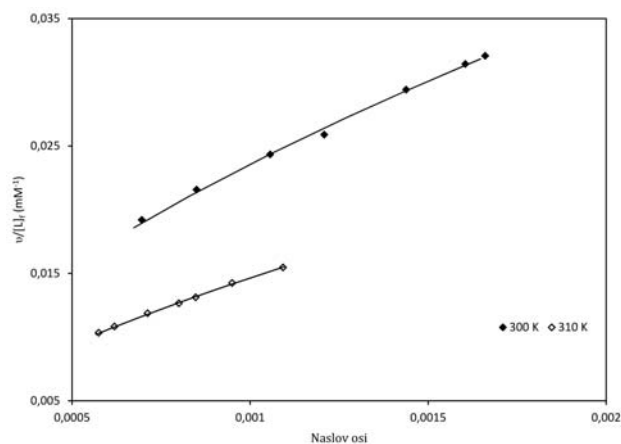


Fig. 5. Scatchard plots for binding of Na[Pd(8-QO)(mal)] to DNA (experimental (dots) and theoretical (lines)).

Table 1. Thermodynamic parameters of DNA interaction with palladium(II) complex

Compound	Temperature (K)	$[L]_{1/2}$ (mM)	$m$ (kJ/mol) (mmol/L) <sup>-1</sup>	$\Delta H^\circ_{(H_2O)}$ (kJ/mol)	$\Delta H^\circ_{(H_2O)}$ (kJ/mol)
Na[Pd(8-Q)(mal)]	300	0.190	90.82	18.51	24.08
	310	0.182	92.00	18.32	

**Table 2.** Values of  $\Delta A_{\max}$  and binding parameters in the Hill equation for interaction between Pd(II) complex and DNA in 20 mmol/L Tris–HCl buffer and pH 7.0

Compound	Temperature (K)	$\Delta A_{\max}$	g	$K \times 10^3 \text{ (M)}^{-1}$	n	Error $\times 10^{-5}$
Na[Pd(8-Q)(mal)]	300	0.007	2	1.140.2	2.510.2	6
	310	0.009		0.920.1	2.750.1	1

indicates noncooperative,  $n > 1$  is cooperative and  $n < 1$  shows anti-cooperative binding of ctDNA with metal complex),  $g$  is the number of binding sites per 1000 nucleotides of ctDNA and  $K$  is apparent binding constant. The theoretical values of these parameters were deduced using Eureka software (Table 2). The values of  $n$  indicated that the Pd(II) complex bind to ctDNA cooperatively, thus, the binding at one site increases the affinity of binding at the other sites and have a series of two binding site.<sup>41</sup> The apparent binding constants of the Pd(II) complex were obtained and are higher than other metal complexes such as [Ru(bpy)<sub>2</sub>(maip)](ClO<sub>4</sub>)<sub>2</sub>  $2.3 \cdot 10^3 \text{ M}^{-1}$  and C<sub>6</sub>H<sub>24</sub>N<sub>4</sub>O<sub>6</sub>CuSn<sub>2</sub>Cl<sub>6</sub>  $4.75 \cdot 10^4 \text{ M}^{-1}$ .<sup>42,43</sup> It was apparent from Table 2 that the maximum errors between experimental and theoretical values of  $v$  are low.

Finding the area under  $v$  versus  $\ln[L]_f$  plot and using Wyman-Jons equation (Eq. 9),<sup>44</sup> we can calculate the  $K_{\text{app}}$  at 300 K and 310 K for each particular  $v$ .

$$S_{V_i} = \ln \left[ 1 + K_{\text{app}} [L]_f^{V_i} \right] \quad (9)$$

Then the binding enthalpy ( $\Delta H^\circ$ ) process can be observed using the van't Hoff equation.<sup>44</sup>

$$\ln (K_2/K_1) = -\Delta H_{\text{binding}} / R (1/T_1 - 1/T_2) \quad (10)$$

Plots of the values of  $\Delta H^\circ$  versus the values of  $[L]_f$  are shown in Fig. 6 for Na[Pd(8-QO)(mal)] complex at 300 K. Deflections are observed in the plot which may be due to binding of metal complex to ctDNA or denatura-

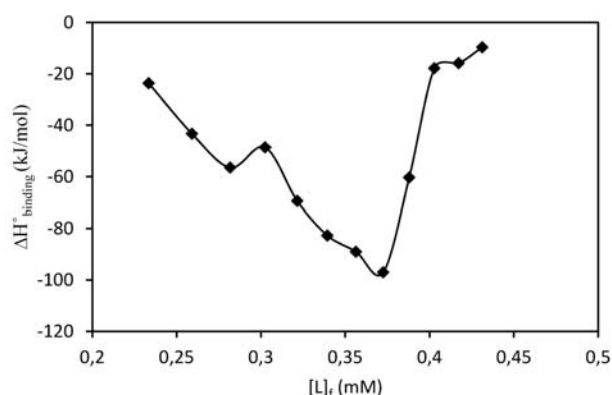


**Fig. 6.** Molar enthalpy of binding in the interaction between DNA and Na[Pd(8-QO)(mal)] versus free concentrations of complex at pH 7.0 and 300 K.

tion of ctDNA. Similar observations can be seen in the literature where Pd(II) and Pt(II) complexes have been interacted with ctDNA.<sup>45,46</sup>

### 3. 5. Fluorescent Spectral Studies

EB emits intense fluorescence in the presence of ctDNA due to its strong intercalation between the adjacent ctDNA base pairs. The addition of a second molecule could quench this enhanced fluorescence.<sup>13,47,48</sup> Hence, competitive ethidium bromide (EB) binding studies were undertaken to gain support for the extent of binding of palladium (II) complexes with ctDNA.

Figure 7 illustrates the fluorescence emission spectra of DNA-EB system with increasing concentrations of the Pd(II) complex. The observed significant reduction in the fluorescence intensity suggested that the complex could bind to ctDNA.

It is well known that fluorescence quenching mechanism can be classified as dynamic quenching and static quenching. Dynamic quenching refers to a process that the fluorophore and the quencher come into contact during the transient existence of the excited state, while static quenching refers to fluorophore–quencher complex formation.<sup>1</sup> In order to confirm the quenching mechanism, the Stern-Volmer constant was measured from the equation below:

$$F_0/F = 1 + K_q \tau_0 [L]_t = 1 + K_{SV} [L]_t \quad (11)$$

$F_0$  and  $F$  are the fluorescence intensities of ctDNA in the absence and in the presence of Pd(II) complex, respectively.  $[L]_t$  is the total concentration of quencher (Pd(II) complex,  $[L]$ ),  $K_q$  is the DNA–EB complex quenching rate constant,  $\tau_0$  is the average lifetime of fluorophore in the absence of Pd(II) complex with value of  $10^{-9}$  to  $10^{-7}$  s and  $K_{SV}$  is the Stern–Volmer dynamic quenching constant.<sup>49,50</sup> The  $K_{SV}$  value is obtained from the slope of  $F_0/F$  versus  $[L]_t$  linear plot (inset of Fig. 7). The values of  $K_{SV}$  and  $K_q$  were listed in Table 3. It can be seen that the values of  $K_q$  is far greater than  $2.0 \cdot 10^{10} \text{ M s}^{-1}$ , the maximum diffusion collision quenching rate constant of various quenchers with the biopolymer.<sup>51</sup> This suggests that DNA binding with the Pd(II) complex is a static quenching process.

For static quenching, the binding constant ( $K_b$ ) and number of binding ( $n$ ) were estimated by the following equation.<sup>52,53</sup>

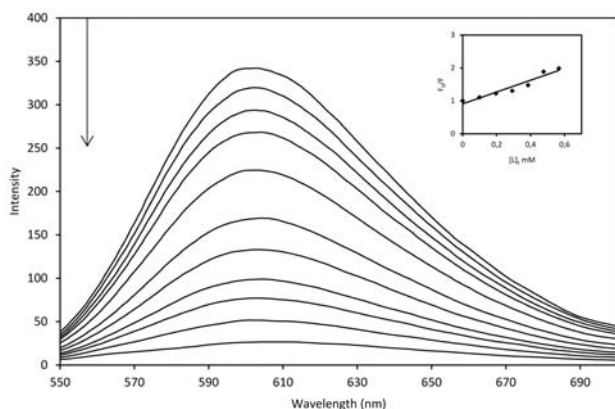


**Fig. 7.** Fluorescence emission spectra of EB-DNA system in the presence of Na[Pd(8-QO)(mal)] complex at 300 K in Tris-HCl buffer, pH 7.0. (Inset, The Stern–Volmer plot for the fluorescence quenching of Na[Pd(8-QO)(mal)] complex by ctDNA at 300 K).

$$\log(F_0 - F)/F = \log K_b + n \log[L]_t \quad (12)$$

According to the equation above the binding parameters can be obtained from the slope of  $1/(F_0 - F)$  against  $1/[L]_t$  at 293, 300 and 310 K (Fig. 8 and Table 3). The number of binding sites for this complex is in good agreement with the above absorption spectral results. In addition, the binding constant was greater than the Stern–Volmer constant, therefore, the probable quenching mechanism of a Pd(II)-DNA-EB binding reaction is initiated

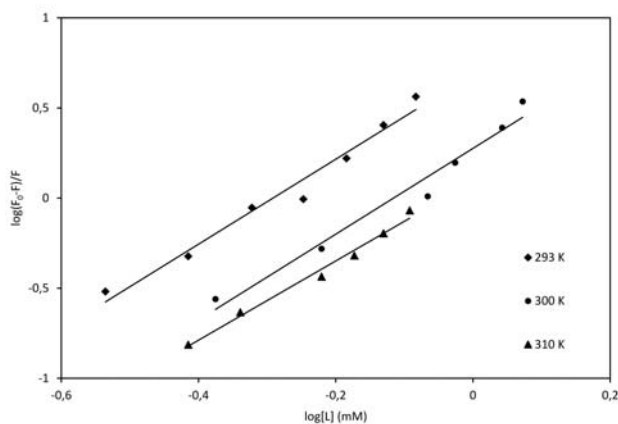


**Fig. 8.** Comparative plot of  $\log(F_0/F)/F$  versus  $\log[L]_t$  for determining the binding constant and number of binding sites of Na[Pd(8-QO)(mal)] complex in Tris-HCl buffer, pH 7.0, at 300 K (◆), 310 K (●) and 320 K (▲).

**Table 3.** Binding parameters for interaction of palladium complex on DNA.

Compound	Temperature (K)	$K_{SV} \times 10^3$ (M) <sup>-1</sup>	$K_a \times 10^{12}$ (Ms) <sup>-1</sup>	$K_b \times 10^3$ (M) <sup>-1</sup>	n	$\Delta G^\circ$ (kJ/mol)	$\Delta H^\circ$ (kJ/mol)	$\Delta S^\circ$ (kJ/molK)
Na[Pd(8-Q)(mal)]	293			$4.86 \pm 0.1$	$2.35 \pm 0.1$	-3.85		
	300	1.080.1	5.80.2	$1.88 \pm 0.2$	$1.79 \pm 0.3$	-1.57	-154.96	-0.49
	310			$1.23 \pm 0.3$	$2.20 \pm 0.2$	-0.53		

by compound formation rather than static quenching.<sup>54</sup> The decreasing trend of  $K_a$  with increasing temperature confirmed that the fluorescence quenching of palladium complex by ctDNA was static quenching.<sup>1</sup> These results were similar to that reported about the interaction of other cationic metal complexes to ctDNA.<sup>55–56,57</sup>

In order to further demonstrate the mode of binding of Pd(II) complex to ctDNA, the fluorescence titration method were carried out according to Scatchard analysis.<sup>58,59,60–61</sup>

$$r/[L]_f = n K_a - r K_a \quad (13)$$

where  $r$  is the moles of ethidium bromide bound per mole of ctDNA,  $[L]_f$  is the molar concentration of the free ethidium bromide,  $n$  is number of binding sites and  $K_a$  is the apparent binding constant.<sup>62</sup> The apparent binding constant at three different concentrations for Pd(II)-DNA-EB interaction is the slope obtained from the respective Scatchard plots. The number of binding sites has been calculated from the ratio of the intercept to the slope obtained from the plot of  $r/C_f$  vs.  $r$ . The fluorescence Scatchard plots obtained for binding of EB to ctDNA in absence (◆) and presence (○, △, ◇) of various concentrations of Pd(II) complex were shown in Figure 9 and the data were summarized in Table 4. As can be seen from the plots a decrease in slope and the intercept resulted upon the addition of the metal complex concentration indicating the hydrogen binding of the complex with the ctDNA. Thus the results obtained from Scatchard plots validate those obtained from emission spectral studies.<sup>63,64–65</sup>

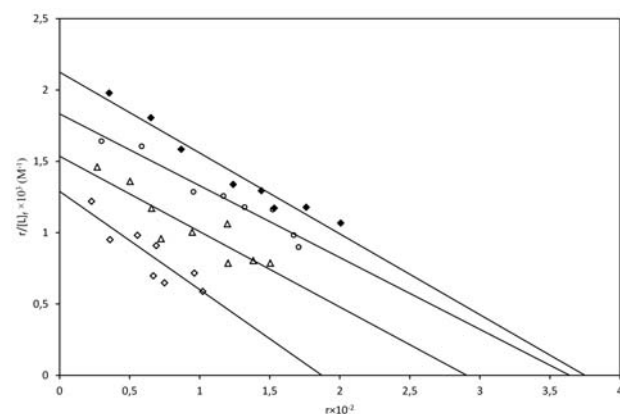


**Fig. 9.** Scatchard plot for the Pd(II)-DNA-EB system at pH 7.



**Table 4.** Binding parameters for the effect of palladium complex on the fluorescence of EB in the presence of DNA.

Compound	$r_f$	$K \times 10^4 \text{ (M)}^{-1}$	$n$
	0.00	$5.31 \pm 0.2$	0.039
Na[Pd(8-Q)(mal)]	3.33	$5.03 \pm 0.2$	0.036
	6.67	$5.28 \pm 0.2$	0.030
	10.00	$6.89 \pm 0.3$	0.019

### 3. 6. Determination of Thermodynamic Parameters

In consideration of the dependence of binding constant ( $K_b$ ) on temperature, a thermodynamic process was considered to be responsible for this interaction.<sup>4</sup>

The thermodynamic parameters of binding reaction are the major evidence for confirming the binding force. The forces acting between a small molecule and macromolecule include hydrogen bond, van der Waals force, electrostatic force, and hydrophobic interaction, among others.<sup>66</sup> If the enthalpy change ( $\Delta H^\circ$ ) does not vary significantly over the temperature range studied, then its value and that of entropy change ( $\Delta S^\circ$ ) can be determined using the modified van't Hoff equation:<sup>67</sup>

$$\ln K = (-\Delta H^\circ/RT) + (\Delta S^\circ/R) \quad (14)$$

The  $\ln K$  versus  $1/T$  plot gave a straight line according to the above equation. The enthalpy and entropy have been obtained from the slope ( $-\Delta H^\circ/R$ ) and intercept ( $\Delta S^\circ/R$ ) of the Van't Hoff plot (Fig. 10) and were presented in Table 3. The Gibbs free energy change values ( $\Delta G^\circ$ ) were calculated from the equation 2 at 293, 300 and 310 K.

Obviously, the binding process is spontaneous because of the Gibbs free energy change value is negative. It is also demonstrated that both enthalpy and entropy changes are negative. These results support the assertion that the binding process was hydrogen and van der Waals binding between Pd(II) complex and ctDNA.<sup>68</sup>

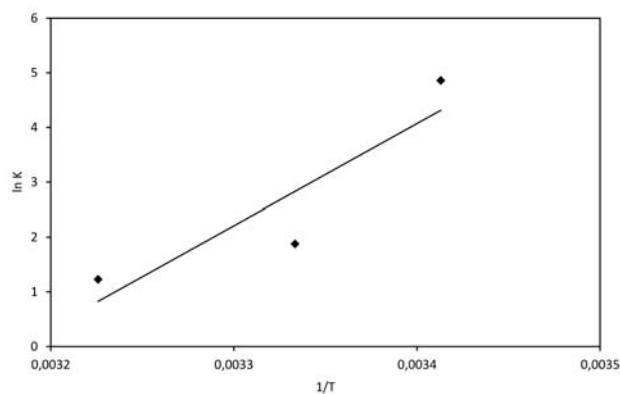


**Fig. 10.** Van't Hoff plot for the binding of Pd(II) complex with DNA.

### 3. 7. Binding Modes

Gel chromatogram is obtained by plotting the absorbance readings at the 260 nm and 376 nm wavelengths versus column fractions. Figure 11 indicates that the peak obtained for the two wavelengths are resolved and suggested the ctDNA has been separated from the metal complex. This implies that the binding between ctDNA and the metal complex is noncovalent under such circumstances. This result further supports our data obtained by fluorescence method. Thus, hydrogen and van der Waals binding seem to play major role in the DNA-complex interaction.<sup>69</sup>

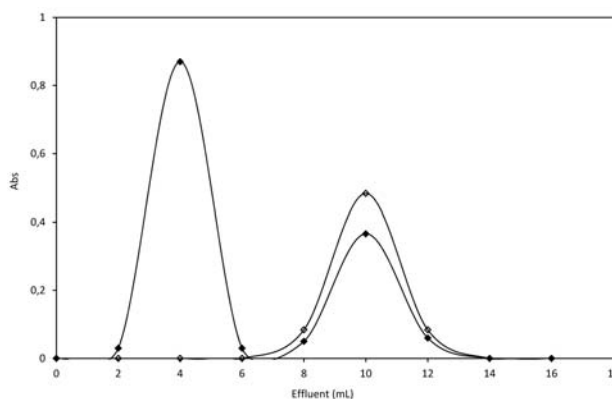


**Fig. 11.** Gel chromatogram of Na[Pd(8-QO)(mal)] obtained on Sephadex G-25 column.

## 4. Conclusion

A new watersoluble palladium(II) complex, Na[Pd(8-QO)(mal)] were designed and synthesized. The effect of this anionic complex on DNA-binding properties and also cytotoxic activities was investigated. The structure of the Pd(II) complex was characterized on the basis of elemental analyses, molar conductivity, FT-IR, UV-Vis and <sup>1</sup>H NMR techniques. The in vitro cytotoxicity studies by MTT assay against human leukemia cell lines, molt, indicated that the complex is moderate activity and indicate possible future improvements. The interactions of the anionic complex with ctDNA were carried out by using absorption spectroscopy, fluorescence titration spectra, Ethidium Bromide displacement and gel chromatography studies. The results suggest that the complex cooperatively interacted with ctDNA at low concentration in the mode of hydrogen and van der Waals binding and quenched the emission intensity of DNA-EB system at different temperatures mainly by static quenching. The results of DNA binding studies of the anionic palladium(II) complex compared with cationic palladium(II) complexes demonstrated that this type of complexes may also be applied to design DNA binding therapeutic molecules and helpful in the development of drug formulation.

## 5. Acknowledgments

We are grateful for the financial support of the Materials and Energy Research Center, University of Sistan and Baluchestan and University of Tehran.

## 6. References

- P. Zhu, G. Zhang, Y. Ma, Y. Zhang, H. Miao, Y. Wu, *Spectrochim Acta A* **2013**, *112*, 7–14.
- A. Kathiravan, R. Renganathan, *Polyhedron* **2009**, *28*, 1374–1378.
- Y. Zhang, G. Zhang, P. Fu, Y. Ma, J. Zhou, *Spectrochim Acta A* **2012**, *96*, 1012–1019.
- R. C. Gupta, G. Spencer-Beach, *Regul. Toxicol. Pharmacol.* **1996**, *23*, 14–21.
- G. Zhang, Y. Ma, *Food Chem.* **2013**, *141*, 41–47.
- N. Akbay, Z. Seferoglu, E. Gök, *J. Fluoresc.* **2009**, *19*, 1045–1051.
- H. Wu, X. Huang, J. Yuan, F. Kou, F. Jia, B. Liu, K. Wang, *Eur. J. Med. Chem.* **2010**, *45*, 5324–5330.
- E. Ramachandran, S. P. Thomas, P. Poornima, P. Kalaivani, R. Prabhakaran, V. V. Padma, K. Natarajan, *Eur. J. Med. Chem.* **2012**, *50*, 405–415.
- N. V. Kulkarni, A. Kamath, S. Budagumpi, V. K. Revankar, *J. Mol. Struct.* **2011**, *1006*, 580–588.
- D. Fregona, L. Giovagnini, L. Ronconi, C. Marzano, A. Trevisan, S. Sitran, B. Biondi, F. Bordin, *J. Inorg. Biochem.* **2003**, *93*, 181–189.
- E. S. Koumoussi, M. Zampakou, C. P. Raptopoulou, V. Psycharis, C. M. Beavers, S. J. Teat, G. Psomas, T. C. Stamatatos, *Inorg. Chem.* **2012**, *51*, 7699–7710.
- J. D. Higgins III, L. Neely, S. Fricker, *J. Inorg. Biochem.* **1993**, *49*, 149–156.
- G. Zhang, Y. Zhang, Y. Zhang, Y. Li, *Sensor. Actuat. B-Chem.* **2013**, *182*, 453–460.
- S. Y. Bi, L. L. Yan, Y. Wang, B. Pang, T. J. Wang, *J. Lumin.* **2012**, *132*, 2355–2360.
- D. Arish, M.S. Nair, *Spectrochim Acta A* **2011**, *82*, 191–199.
- G. Zhang, P. Fu, J. Pan, *J. Lumin.* **2013**, *134*, 303–309.
- S. Y. Bi, L. L. Yan, Y. Wang, B. Pang, T. J. Wang, *J. Lumin.* **2012**, *132*, 2355–2360.
- J. Marmur, *J. Mol. Biol.* **1961**, *3*, 208–218.
- M. E. Reichmann, S. A. Rice, C. A. Thomas, P. Doty, *J. Am. Chem. Soc.* **1954**, *76*, 3047–3053.
- D. Senthil Raja, N. S. P. Bhuvanesh, K. Natarajan, *Inorg. Chim. Acta* **2012**, *385*, 81–93.
- E. Gao, M. Zhu, H. Yin, L. Liu, Q. Wu, Y. Sun, *J. Inorg. Biochem.* **2008**, *102*, 1958–1964.
- W. J. Geary, *Coord. Chem. Rev.* **1971**, *7*, 81–122.
- V. X. Jin, J. D. Ranford, *Inorg. Chim. Acta*, **2000**, *304*, 38–44.
- D. L. Pavia, G. M. Lampman, G. S. Kriz, J. A. Vyvyan, Introduction to Spectroscopy Infrared spectroscopy, Brooks/Cole, Belmont-CA, **2009**, pp. 15–104.
- P. Starha, Z. Travnicek, I. Popa, *J. Inorg. Biochem.* **2009**, *103*, 978–988.
- K. Nakamoto, Infrared and Raman Spectra of Inorganic and Coordination Compounds, Part B: Applications in Coordination, Organometallic and Bioinorganic Chemistry, Wiley, New York, **1997**.
- M. Saeidifar, H. Mansouri-Torshizi, G. Rezaei Behbehani, A. Divsalar, and A. A. Saboury, *Bull. Korean Chem. Soc.* **2009**, *30*, 1951–1955.
- M. Saeidifar, H. Mansouri-Torshizi, A. Divsalar, A. A. Saboury, *J. Iran Chem. Soc.* **2013**, *10*, 1001–1011.
- M. Saeidifar, H. Mansouri-Torshizi, Y. Palizdar, A. Divsalar, A. A. Saboury, *Nucleos. Nucleot. Nucl.* **2013**, *32*, 366–388.
- X. L. Han, F. F. Tian, Y. S. Ge, F. L. Jiang, L. Lai, D. W. Li, Q. L. Yu, J. Wang, C. Lin, Y. Liu, *J. Photochem. Photobiol. B* **2012**, *109*, 1–11.
- Q. Wang, Zh. Yang, G. Qi, D. Qin, *Eur. J. Med. Chem.* **2009**, *44*, 2425–2433.
- H. Mansouri-Torshizi, M. Saeidifar, G. R. Rezaei-Behbehani, A. Divsalar and A. A. Saboury, *J. Chin. Chem. Soc.* **2010**, *57*, 1299–1308.
- F. Greene, C. N. Pace, *J. Biol. Chem.* **1974**, *249*, 5388–5393.
- M. Q. King, B. H. Nicholson, *Biochem. J.* **1969**, *114*, 679–687.
- Z. Bathaie, A. Bolhasani, R. Hoshyar, B. Ranjbar, F. Sabouni, A. A. Moosavi-Movahedi, *DNA Cell Biol.* **2007**, *26*, 533–540.
- G. M. Barrow, Physical Chemistry, MC Graw-Hill, New York, **1988**, pp. 201–216.
- A. Divsalar, A. A. Saboury, L. Ahadi, E. Zemanatiyar, H. Mansouri-Torshizi, *BMB reports* **2010**, *43*, 766–771.
- M. Islami-Moghaddam, H. Mansouri-Torshizi, A. Divsalar, A. A. Saboury, *J. Iran. Chem. Soc.* **2009**, *6*, 552–569.
- G. Scatchard, *Ann. N. Y. Acad. Sci.* **1949**, *51*, 660–672.
- A. V. Hill, *J. Physiol.* **1910**, *40*, 4–7.
- H. Mansouri-Torshizi, M. Saeidifar, A. Divsalar, A. A. Saboury, *Spectrochim. Acta A* **2010**, *77*, 312–318.
- Y. J. Liu, C. H. Zeng, H. L. Huang, L. X. He, F. H. Wu, *Eur. J. Med. Chem.* **2010**, *45*, 564–571.
- F. Arjmand, F. Sayeed, *J. Mol. Struct.* **2010**, *965*, 14–22.
- H. Mansouri-Torshizi, M. Islami-Moghaddam, A. A. Saboury, *Acta Biochim. Biophys. Sin.* **2003**, *35*, 886–890.
- M. Islami-Moghaddam, H. Mansouri-Torshizi, A. Divsalar, A. A. Saboury, *J. Iran Chem. Soc.* **2009**, *6*, 552–569.
- H. Mansouri-Torshizi, M. Islami-Moghaddam, A. Divsalar, A. A. Saboury, *Acta Chim. Slov.* **2011**, *58*, 811–822.
- R. Gaur, L. Mishra, *Inorg. Chem.* **2012**, *51*, 3059–3070.
- Q. Guo, L. Li, J. Dong, H. Liu, T. Xu, J. Li, *Spectrochim. Acta A* **2013**, *106*, 155–162.
- S. Bi, H. Zhang, C. Qiao, Y. Sun, C. Liu, *Spectrochim. Acta A* **2008**, *69*, 123–129.
- J. R. Lakowica, G. Weber, *Biochemistry* **1973**, *12*, 4161–4170.
- W. R. Ware, *J. Phys. Chem.* **1962**, *66*, 455–458.
- P. Krishnamoorthy, P. Sathyadevi, A. H. Cowley, R. R. Butorac, N. Dharmaraj, *Eur. J. Med. Chem.* **2011**, *46*, 3376–3387.

53. F. Xue, C. Z. Xie, Y. W. Zhang, Z. Qiao, X. Qiao, J. Y. Xu, S. P. Yan, *J. Inorg. Biochem.* **2012**, *115*, 78–86.
54. L. W. Zhang, K. Wang, X. X. Zhang, *Anal. Chim. Acta* **2007**, *603*, 101–110.
55. G. Zhang, X. Hu, P. Fu, *J. Photochem. Photobiol. B* **2012**, *108*, 53–61.
56. F. Xue, C. Z. Xie, Y. W. Zhang, Z. Qiao, X. Qiao, J. Y. Xu, S. P. Yan, *J. Inorg. Biochem.* **2012**, 78–86.
57. H. Wu, J. Yuan, Y. Bai, G. Pan, H. Wang, X. Shu, *J. Photochem. Photobiol. B* **2012**, *107*, 65–72.
58. L. Guo, B. Qiu, G. Chen, *Anal. Chim. Acta* **2007**, *588*, 123–130.
59. C. V. Kumar, J. K. Barton, N. J. Turro, *J. Am. Chem. Soc.* **1985**, *107*, 5518–5523.
60. F. Wu, Y. Xiang, Y. Wu, F. Xi, *J. Lumin.* **2009**, *129*, 1286–1291.
61. A. Ray, B. Koley Seth, U. Pal, S. Basu, *Spectrochim. Acta A* **2012**, *92*, 164–174.
62. J. B. Lepecq, C. Paoletti, *J. Mol. Biol.* **1967**, *27*, 87–106.
63. P. R. Reddy, A. Shilpa, N. Raju, P. Raghavaiah, *J. Inorg. Biochem.* **2011**, *105*, 1603–1612.
64. H. Mansouri-Torshizi, T. S. Srivastava, S. J. Chavan, M. P. Chitnis, *J. Inorg. Biochem.* **1992**, *48*, 63–70.
65. A. K. Paul, H. Mansouri-Torshizi, T. S. Srivastava, S. J. Chavan, M. P. Chitnis, *J. Inorg. Biochem.* **1993**, *50*, 9–20.
66. S. S. Wu, W. B. Yuan, H. Y. Wang, Q. Zhang, M. Liu, K. B. Yu, *J. Inorg. Biochem.* **2008**, *102*, 2026–2034.
67. Y. Zhang, G. Zhang, P. Fu, Y. Ma, J. Zhou, *Spectrochim. Acta A* **2012**, *96*, 1012–1019.
68. B. Hemmateenejad, M. Shamsipur, F. Samari, T. Khayamian, M. Ebrahimi, Z. Rezaei, *J. Pharmaceutical and Biomedical Analysis* **2012**, *67–68*, 201–208.
69. H. Mansouri-Torshizi, T. S. Srivastava, H. K. Parekh, M. P. Chitnis, *J. Inorg. Biochem.* **1992**, *45*, 135–148.

## Povzetek

Nov anionski 8-hidroksikinolinatopaladati(II) kompleks z malonatom je bil sintetiziran in okarakteriziran z elementno analizo, prevodnostjo, FT-IR, UV-Vis in  $^1\text{H}$  NMR tehnikami z namenom nadaljevati z razvojem proti-rakavih sredstev. Citotoksičnost je bila določena na človeških levkeminih celicah z MTT analizo. Z novim antitumornim Pd(II) kompleksom je bila testirana tudi njegova vezava na ctDNA v fiziološkem pufru (pH 7.0) z uporabo absorpcijske spektroskopije, fluorescenčnega titracijskega spektra, z zamenjavo etidijevega bromida in gelske kromatografije. Pridobljeni rezultati nakazujejo, da se vodotopni kompleks ve e na DNA preko mehanizma statičnega ugašanja pri nizki temperaturi. Termodinamski parametri pridobljeni s fluorescenčnimi eksperimenti pri različnih temperaturah poka ejo, da pri procesu vezave sodelujejo vodikove vezi in van der Waalove sile, kar dokazujejo Scatchardovi diagrami.